Separatrix eigenfunctions

John R. Cary* and Petre Rusu†
Department of Physics, University of Colorado, Boulder, Colorado 80309-0390
(Received 7 November 1990; revised manuscript received 20 February 1992)

Near-separatrix eigenfunctions for the double-well potential are analyzed. These functions are needed for the study of systems with perturbed or slowly varying double-well potentials. The probability density of separatrix eigenfunctions collapses to the classical result (a δ function at the unstable fixed point) logarithmically with the number of quantum states. Matrix elements with respect to this basis are also studied. Unlike the wave functions, the unnormalized matrix elements are nonsingular in the limit of large quantum number.

PACS number(s): 03.65.Sq, 03.65.Ge

I. INTRODUCTION

Recent advances in nonlinear dynamics have shown the richness of classical Hamiltonian motion [1,2]. Besides the well-known integrable (or regular) systems, such as the Kepler system and the pendulum, there exist systems with chaos. This chaos is manifest in the mixing of phase space by the flow, the sensitivity of trajectories to initial conditions, and the slow diffusion of approximate invariants due to perturbations. Quantum chaos is concerned with the manifestation of chaos in quantum systems that are chaotic in the classical analysis. (A review of these matters is given by Zaslavskii [3].) It has been found that the eigenvalues of classically chaotic systems can be sensitive [4,5] to perturbations and that the eigenvalue distribution offers substantially [6,7] from cases where the classical system is integrable. Such quantum systems also may have irregular wave functions [8]. Quantum effects can also mitigate chaos by, for example, eliminating momentum diffusion in maps [9,10].

Perturbations to an integrable classical system affect the separatrix immediately. An example is the Hamiltonian $H=\frac{1}{2}p^2+V(x)$ for nonrelativistic, one-dimensional motion in a potential with a local maximum. [A *symmetric double-well* potential is shown in Fig. 1(a). The phase-space contours of the Hamiltonian are shown in Fig. 1(b). In general, the potential will not be symmetric in our analysis.] Upon application of a time-periodic perturbation, the unstable fixed point becomes an unstable periodic point. Melnikov's analysis [11] shows that a homoclinic tangle arises generically in the vicinity of this unstable periodic point. This implies the nonexistence of an analytic invariant in this region.

Because of its sensitivity to chaos-inducing perturbations, the separatrix is a fruitful area for the study of quantum chaos. In fact, quantum effects for wave functions with energies near that of a local barrier maximum have already been studied extensively in the semiclassical limit. (Reference [12] is a review of semiclassical methods.) The transmission coefficient, given by the standard tunneling factor for energies well below the local maximum, is also less than unity for energies near to but above the local maximum [13]. Moreover, the local maximum causes a phase shift [14] between the incident and transmitted waves. The effects of this phase shift on the eigenvalues of the symmetric double-well potential were calculated in Ref. [14]. Both the phase shift (recognized in Ref. [15] and included in Ref. [16]) and the modification of the transmission factor are important in determining the bound-state energies of a general (asymmetric) double-well potential. (Earlier work [17] had discussed the effects of the tunneling factor alone.) The accuracy of these and higher-order semiclassical results [18] have been checked [19] by comparison with numerical calculations. In later work [20] the results of Ref. [16] were combined with general formulas [21] for the classical actions near a separatrix to determine the behavior of near-separatrix quantum excitation frequencies in the semiclassical limit.

For a complete picture, the structure of wave functions, their associated normalization factors, and methods for calculating matrix elements are needed in the semiclassical limit. Yngve [22] showed that normalization factors for the wave functions could be obtained by combining a result of Furry [23] with known formulas for the transmission coefficient and phase shift. However, matrix elements seem to have been calculated only for states well below or well above the barrier [24].

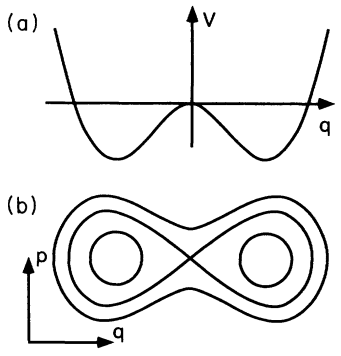

FIG. 1. (a) The double-well potential of the analysis. (b) The classical phase space showing the contours of the Hamiltonian for the potential (a).

The goals of the present work are to study further the structure of near-separatrix excitation frequencies and wave functions and to provide methods for calculating matrix elements between quantum states near the barrier top in the semiclassical limit. For this reason we briefly review the semiclassical analysis of the double-well potential in Sec. II. In this section we rederive the matching coefficients in preparation for our analysis of the relative probabilities for the regions near the barrier and far from the barrier. In addition, we examine the behavior of the excitation frequencies for asymmetric potentials, as Ref. [20] was restricted to symmetric potentials.

With the wave functions in hand we proceed to discuss the normalization in Sec. III. As mentioned above, normalized wave functions were obtained previously [22]. However, we present another derivation, a direct integration by matched asymptotics of the semiclassical wave functions. This approach allows us to calculate explicitly the contributions to the probability from the various regions, e.g., classically allowed and near the barrier, so that we can show how the classical probability density is obtained as $\hbar \to 0$. In this process, we express the normalization factor in terms of the WKB amplitudes in the classically allowed regions, which is more natural for taking the classical limit. Finally, in Sec. IV we show how to calculate the matrix elements for the near-separatrix eigenfunctions.

It has previously been noted that the classical excitation frequency is obtained very slowly in the limit of large quantum number. In the classical system the excitation frequency is the orbit frequency. Perturbations at the frequency of the orbit drive the motion resonantly. In quantum systems the excitation frequency is the frequency difference between quantum states. Perturbations at the frequency difference give rise to transitions from one quantum state to the other. The quantum excitation frequency is known to approach the classical excitation frequency in the limit of small Planck's constant ($\hbar \to 0$) or, equivalently, large quantum number ($N \to \infty$). However, for the case of systems with separatrices this limit is approached very slowly. In this classical system the minimum excitation frequency is zero, which is the frequency on the separatrix. However, in the quantum system, the minimum frequency close to the separatrix is of the order of $\omega_0/\ln|N|$ (equivalently $\omega_0/\ln|1/\hbar|$), where ω_0 is a typical classical frequency. It has been suggested [20] that this slow approach to the classical limit may provide a means for observing quantum effects in systems with very large ($\approx 10^6$) numbers of quantum states.

Here we find that the classical probability density is also obtained slowly in the limit of large quantum number. However, this limit is more complicated. The classical probability, essentially the time of sojourn in a given region, collapses to a δ function on the unstable fixed point for the separatrix. Thus, the probability density at the unstable fixed point is infinite. Moreover, the total probability of being inside an arbitrarily small interval $[-\delta,\delta]$ around the unstable fixed point is unity, and, so, the probability of being found away from the fixed point is zero. For the quantum system with a large number of quantum states, the probability density at the origin diverges as $1/\hbar^{1/2}$. This indicates that the peak probability density diverges rapidly (that is to say, converges rapidly to ∞) in the classical limit. However, the classical probability of being far from the separatrix falls to zero only logarithmically with $\hbar$. Thus, the separatrix wave functions become peaked very rapidly as $\hbar \to 0$, but the vanishing of the probability of being far from the fixed point occurs very slowly.

Our analysis is geared in particular towards determining the elements needed for an analysis of the breakdown of quantum adiabatic invariance theory for systems that have a classical separatrix. This system is of particular interest because of the recent results that show explicitly how the classical adiabatic invariant is lost in such systems. Numerical experiments [25] indicate that the region of phase space swept by the separatrix is ergodic in the limit $\epsilon \to 0$. Analytic calculations for special cases [26,27] and in general [21,28] show that an ensemble of orbits originally on one contour of the adiabatic invariant is spread over an annulus of contours after the separatrix crossing has taken place. The characteristic width of this annulus scales linearly with the adiabatic parameter ϵ in the symmetric case and as $\epsilon \ln|1/\epsilon|$ in the general case.

The results derived here have been used elsewhere in the analysis of the adiabatically varied quantum system. With the presently derived matrix elements a transformation to the rotating-axis representation [29] may be effected. This rotating-axis transformation allows the behavior of adiabatic invariant loss to be determined [30] for the quantum system in the limit of small ϵ. The rotating-axis equations may also be integrated numerically [31] to determine the differences between quantum and classical analyses far from the quantum adiabaticity threshold.

Possible applications of this analysis are to the Penning trap [32], optical wave guides [33], and the study of separatrix states in higher-dimensional systems [34]. The usual Penning trap would have to be modified to produce a separatrix in the longitudinal motion. This might be effected by introducing five ring electrodes, with the center one and outer two biased to repel, while the intermediate electrodes are biased to attract. Schrödinger's equation, derived via the paraxial approximation, is valid for optical waveguides formed by modification of a dielectric substrate. The longitudinal propagation coordinate takes the place of time. Double-well potentials for the transverse motion occur when the dielectric profile is modified to split one wave guide into two.

II. SEMICLASSICAL ANALYSIS OF THE DOUBLE-WELL POTENTIAL

The normalization factors and probabilities are integrals over all or part of space of the modulus of the wave function. Thus, a first step is to obtain the wave functions. Though this was in essence carried out previously, we present elements of this analysis in order to introduce our notation and to collect the needed formulas in one place. We carry out this analysis with patched uniform approximations [12,35,36]. We note the characteristic size of the wave function in the various regions

and provide a more detailed discussion of the characteristic behavior of the quantum excitation frequency for near-separatrix wave functions for the asymmetric case.

A. Review of the uniform approximation

The goal of semiclassical theory is to solve the time-independent Schrödinger equation,

$$\hbar^2\frac{d^2\phi}{dx^2}=Q(x)\phi\ , \tag{1}$$

in the limit of small $\hbar$, or large mode number. In this equation,

$$Q(x)\equiv -p^2(x)\ , \tag{2a}$$

where

$$p(x)\equiv\sqrt{2m[E-V(x)]} \tag{2b}$$

is defined to be the momentum of a particle of energy E at position x. For classically forbidden regions, the convention is chosen that p is positive imaginary.

The idea of the uniform approximation is to transform to a *comparison equation,*

$$\hbar^2\frac{d^2\chi}{d\xi^2}=F(\xi)\chi(\xi)\ , \tag{3}$$

for which the solution is known. For new and old functions related by

$$\phi(x)=f(x)\chi(\xi) \tag{4}$$

and with the choice,

$$f(x)=\left[\frac{d\xi}{dx}\right]^{-1/2}\ , \tag{5}$$

the relation between the new and old dependent variables is

$$\left[\frac{d\xi}{dx}\right]^2=\frac{Q}{F}-\frac{\hbar^2}{F}\left[\frac{d\xi}{dx}\right]^{1/2}\frac{d^2}{dx^2}\left[\frac{d\xi}{dx}\right]^{-1/2}\ . \tag{6}$$

Neglecting the last term in this equation gives the lowest-order (in $\hbar$) differential equation for the transformation between the two independent variables. In this case, the solution for the original problem is found to be given by

$$\phi(x)=\{F[\xi(x)]/Q(x)\}^{1/4}\chi[\xi(x)]\ . \tag{7}$$

Examination of Eq. (6) indicates a possible problem at turning points, the zeros of Q. At such zeros, F must also vanish for the first term on the right side of Eq. (6) to be finite. Thus, F and Q have zeros at equivalent points. In addition, the second term on the right side of Eq. (6) must not diverge, which it might without further consideration, since it contains F as a divisor, without a compensating factor of Q. As shown by Pechukas [36], arbitrariness in the choice of a particular solution to Eq. (5) allows a nondivergent solution for $\xi(x)$ to be found. Pechukas further showed that for such a solution, the comparison equation has the same classical action integral (or quantum tunneling factor for forbidden regions) between turning points. We will see this in our analysis of the eigenfunction in the region near the barrier.

In the case of a single turning point, the comparison equation is the Airy equation, for which the solutions are known. For two turning points, the comparison equation is the parabolic cylinder equation, which again has been extensively analyzed. However, in the present case there can be four turning points. A possible comparison potential is a quartic polynomial. However, for such a potential, full solutions are not known. Hence, we must still asymptotically patch together solutions valid in separate regions. This implies that our solutions will be valid only if the barrier is well separated from the outer turning points.

These regions are illustrated in Fig. 2. In regions 1 and 3, there is a single turning point, so the Airy function solution is valid. In region 2, the parabolic cylinder solutions are valid [37,38]. Matching will take place in the overlap regions, where both approximations are valid [12,35,39]. The overlap region of, for example, regions 1 and 2 is that region far from the barrier, yet not close to the left turning point.

B. Outer solutions

The solutions in regions 1 and 3 are found by using the Airy equation as a comparison equation. These solutions decay in the classically forbidden region, are basically Airy functions near the turning points, and are the usual rapidly varying phase solutions in the classically allowed regions. For present purposes, we need only the rapidly varying phase solutions. These are (cf. Refs. [12] and [39])

$$\phi(x)\approx\phi^{\text{rp}}_{\mp}(x)$$
$$=A_-|p(x)|^{-1/2}\sin\left[\hbar^{-1}\int_{x_-}^{x}p(y)dy+\pi/4\right] \tag{8a}$$

in the overlap of regions 1 and 2, and

$$\phi(x)\approx\phi^{\text{rp}}_{\mp}(x)$$
$$=A_+|p(x)|^{-1/2}\sin\left[\hbar^{-1}\int_{x}^{x_+}p(y)dy+\pi/4\right] \tag{8b}$$

in the overlap of regions 2 and 3. The points x_- and x_+ appearing in these equations are the outer turning points shown in Fig. 2.

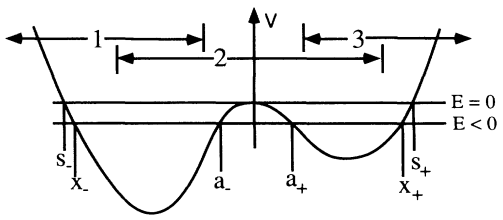

FIG. 2. The regions for the analysis via asymptotic matching. The outer turning points for zero and arbitrary energy as well as the inner turning points for negative energy are labeled.

C. Solution near the barrier

For simplicity we assume that the barrier maximum occurs at $x=0$, at which point the potential vanishes:

$$V(x)=0 \tag{9a}$$

and

$$\frac{dV}{dx}(0)=0 . \tag{9b}$$

We denote the value of the second derivative of the potential at the maximum by

$$b\equiv -\frac{d^2V}{dx^2}(0) . \tag{10}$$

The solution in region 2 is found by comparing with the parabolic cylinder functions, which satisfy the equation,

$$\hbar^2\frac{d^2\chi}{d\xi^2}+(\nu+\tfrac{1}{4}\xi^2)\chi=0 . \tag{11}$$

A further scaling, $\xi=\sqrt{\hbar}\eta$, shows that the solutions to this equation are linear combinations of parabolic cylinder functions, $W(-\gamma,\eta)$ and $W(-\gamma,-\eta)$ (See Ref. [40], Sec. 19.16), where

$$\gamma\equiv\nu/\hbar . \tag{12}$$

Thus, the uniform approximation gives the solution,

$$\phi(x)=\frac{(\gamma+\frac{1}{4}\eta^2)^{1/4}}{Q^{1/4}}[CW(-\gamma,\eta)+DW(-\gamma,-\eta)] . \tag{13}$$

When there are interior turning points, the value of γ is determined by integrating Eq. (6) (keeping only the lowest-order term) between the turning points. This condition,

$$\int_{-2|\hbar\gamma|^{1/2}}^{2|\hbar\gamma|^{1/2}}d\xi\sqrt{|\hbar\gamma|-\tfrac{1}{4}\xi^2}=\int_{x_-}^{x_+}dx\sqrt{Q(x)} ,$$

a statement that the tunneling factors have to be equal in the original system and the comparison system, determines that

$$\gamma=-\frac{1}{\pi\hbar}\int_{x_-}^{x_+}dx\sqrt{2m[V(x)-E]} . \tag{14}$$

We are considering states with energies near that of the barrier. Otherwise, for positive energy the large tunneling factor effectively prevents communication between the two sides of the potential barrier. In this case we can shrink region 2 to be a small region around the barrier maximum and approximate $V(x)$ arbitrarily well by a parabola in this region. Then Eq. (14) becomes

$$\gamma=E/\hbar\omega_0 , \tag{15}$$

where $\omega_0\equiv\sqrt{b/m}$ is the classical rate of exponential separation for trajectories near the barrier. It is also the harmonic-oscillator frequency obtained for the inverted potential. In this region the original equation and the comparison equations have the same form, so we can take η and ξ to be proportional to x:

$$\frac{dx}{d\xi}=\frac{x}{\xi}=\frac{\sqrt{\nu+\frac{1}{4}\xi^2}}{\sqrt{2mE+mbx^2}} .$$

This implies that the proportionality is

$$\eta=\Lambda x\equiv\sqrt{2m\omega_0/\hbar}\,x . \tag{16}$$

For positive energy, the parameter γ is not determined by the uniform approximation. The reason is that for fixed energy, the rapidly varying phase approximation without turning points becomes arbitrarily good in the limit of vanishing $\hbar$. However, we are interested in the case where the energy scales with $\hbar$, because we want to understand states within a few quanta of the barrier energy. In this case, we use the same comparison equation as before.

D. Matching inner and outer solutions

The relation between the coefficients A_- and A_+ of Eqs. (8) and C and D of Eq. (13) is determined by the matching condition: The two solutions must agree in the overlap region. The overlap region is that which is close enough to the center so that the potential can be approximated by a parabola, yet sufficiently far from the interior turning points so that the rapidly varying phase solutions (8) are valid. The first condition is simply $x\ll s_\pm$. The second condition follows from the discussion of Sec. 10.2 of Ref. [39]. For the present case of near-separatrix eigenfunctions, this condition is

$$\hbar^{1/2}/(mb)^{1/4}\ll x .$$

Thus, the matching region is

$$\hbar^{1/2}/(mb)^{1/4}\ll x\ll s_\pm . \tag{17}$$

Such matching has been carried out before [12,16], so we will not repeat the details. The results are

$$C=A_+\cos(\theta_+)/\hbar^{1/4}\kappa^{1/2}$$
$$=\kappa^{1/2}A_-\sin(\theta_-)/\hbar^{1/4} , \tag{18a}$$

and

$$D=\kappa^{1/2}A_+\sin(\theta_+)/\hbar^{1/4}$$
$$=A_-\cos(\theta_-)/\hbar^{1/4}\kappa^{1/2} , \tag{18b}$$

where

$$\kappa\equiv\sqrt{1+\exp(-2\pi\gamma)}-\exp(-\pi\gamma) , \tag{19a}$$

$$\theta_\pm\equiv\pi I_\pm/h-\varphi/2 , \tag{19b}$$

and

$$\varphi\equiv\gamma(1-\ln|\gamma|)+\arg[\Gamma(\tfrac{1}{2}+i\gamma)] . \tag{20}$$

The quantities

$$I_\pm\equiv 2\left|\int_{x_\pm}^{a_\pm}dy\sqrt{2m[E-V(y)]}\right| \tag{21}$$

are the classical action integrals. The lower bound is the

location of the barrier maximum when the energy is negative, and it is zero when the energy is positive.

E. The quantum energy levels

The quantum energy levels come from the fact that Eqs. (18) imply two values for the ratio A_-/A_+:

$$\frac{A_-}{A_+}=\frac{\cos(\theta_+)}{\kappa\sin(\theta_-)}=\frac{\kappa\sin(\theta_+)}{\cos(\theta_-)} . \tag{22}$$

Equating these two expressions yields [16] the equation,

$$\cot(\theta_-)\cot(\theta_+)=\kappa^2 =e^{2\pi\gamma}/[1+(1+e^{2\pi\gamma})^{1/2}]^2 , \tag{23}$$

which was also noted in Ref. [41]. Here we discuss this equation in more detail to determine the scaling of the excitation energy of states with energies near the barrier maximum. The symmetric case was analyzed previously in Ref. [20]. In this discussion we will make use of an alternate form

$$\cos(\theta_T)=-\cos(\theta_\Delta)/(1+e^{2\pi\gamma})^{1/2} , \tag{24}$$

for which

$$\theta_T\equiv\theta_++\theta_-=\pi I_T/h-\varphi\equiv\pi(I_++I_-)/h-\varphi \tag{25a}$$

and

$$\theta_\Delta\equiv\theta_+-\theta_-=\pi I_\Delta/h\equiv\pi(I_+-I_-)/h . \tag{25b}$$

Either Eq. (23) or (24) may be solved for the allowed energy values.

For large negative γ (states trapped deeply below the barrier maximum) the right side of Eq. (23) vanishes. Thus, the eigenvalues for deeply trapped states are given by the two sequences of roots,

$$\cos(\theta_\pm)=0 . \tag{26}$$

Since

$$\lim_{|\gamma|\to\infty}\varphi=0 , \tag{27}$$

these two sequences correspond to

$$I_\pm=(n+\tfrac{1}{2})h , \tag{28}$$

the familiar result that the action is quantized in units of Planck's constant. The two sequences of Eq. (26) or (28) correspond to wave functions trapped on either side of the barrier. When the two sequences predict a degeneracy, the states are no longer localized [6,42] to one side of the barrier, and the splitting of the degeneracy is determined by the right side of Eq. (23). Indeed, when the system is symmetric, so that $I_+=I_-$, the states have definite parity, so that the probabilities for being in either half of the well are identical.

For large, positive γ the right side of Eq. (24) vanishes. In this case, the quantum levels are given by

$$\cos(\theta_T)=0 , \tag{29a}$$

or

$$I_T=(n+\tfrac{1}{2})h , \tag{29b}$$

again the usual result.

To analyze the case $\gamma=O(1)$, it is necessary to know the behavior of the classical action near the separatrix, i.e., for small E. According to Ref. [21], near the separatrix the classical action is given by

$$I_\pm=Y_\pm+E(1+\ln|E_\pm/E|)/\omega_0 , \tag{30}$$

for either sign of E. The quantities $Y_\pm$ in this equation are the phase-space area enclosed by the lobes of the separatrix. Similarly, $Y_T\equiv Y_++Y_-$, and $Y_\Delta\equiv Y_+-Y_-$. The positive quantities $E_\pm$ are of the order of typical energies of the system, such as the depths of the wells. These quantities are given in Ref. [21] for a general Hamiltonian. For the present case, where the Hamiltonian is the sum of the usual kinetic energy $p^2/2$ and a potential energy depending on only the position, the quantities $E_\pm$ are given by

$$\ln(E_+/2bs_+^2)=2\int_0^{s_+}dx\left[\left|\frac{b}{2V(x)}\right|^{1/2}-\frac{1}{x}\right] . \tag{31}$$

The classical actions (30) are finite near the separatrix, but their derivatives $T_\pm(E)\equiv\partial I_\pm/\partial E=\ln|E_\pm/E|/\omega_0$ diverge. This occurs because this derivative is the classical orbit period, which is infinite on the separatrix, since the separatrix contains a fixed point.

Far from the separatrix, Eqs. (28) and (29) show that the energy separation is given by $\Delta I_\rho=h$, where $\rho=\pm$ or T as appropriate. Taylor expansion thus gives the typical energy-level separation as

$$\Delta E_\rho/h=2\pi/T_\rho . \tag{32}$$

That is, the quantum frequency separation is the classical orbit frequency. This is the standard result of semiclassical theory. (For negative-energy states this analysis neglects the possible degeneracies mentioned earlier.)

To determine the typical frequency separation near the separatrix, we combine Eqs. (24) and (30) to obtain

$$\cos\{\pi N_T+\gamma\ln|\gamma_T|-\arg[\Gamma(\tfrac{1}{2}+i\gamma)]\} =-\frac{\cos[\pi N_\Delta+(\gamma/2)\ln|\gamma_+/\gamma_-|]}{\sqrt{1+\exp(2\pi\gamma)}} , \tag{33}$$

in which

$$N_\rho=Y_\rho/h \quad \text{for } \rho=\pm,\ T,\ \text{or } \Delta \tag{34a}$$

are the various separatrix actions in units of Planck's constant,

$$\gamma_\rho\equiv E_\rho/\hbar\omega_0 \quad \text{for } \rho=\pm \tag{34b}$$

and

$$\gamma_T\equiv(\gamma_+\gamma_-)^{1/2} . \tag{34c}$$

The quantities γ_ρ are of the order of the number of trapped quantum states N_ρ and, hence, are large in the semiclassical limit, since they are ratios of macroscopic energies to the energy of one quantum.

For $\gamma \lesssim 1$, Taylor expansion of the Γ function is used. This yields

$$\cos\{\pi N_T+\gamma[\ln|\gamma_T|-\psi(\tfrac{1}{2})]\} = -\frac{\cos[\pi N_\Delta+(\gamma/2)\ln|\gamma_+/\gamma_-|]}{\sqrt{1+\exp(2\pi\gamma)}} \quad (35)$$

in which ψ is the digamma function. In the limit of large $\ln|\gamma_T|$ the right side of Eq. (35) is a slowly varying function compared with the left side. Furthermore, the right side is always less than unity in magnitude. Hence, there is one solution of Eq. (35) in each half-period of the left side of this equation. Therefore, the typical spacing of eigenvalues near the separatrix is given by

$$\Delta\gamma \approx \pi/[\ln|\gamma_T|-\psi(\tfrac{1}{2})] \quad (36a)$$

or

$$\Delta E/\hbar \approx \pi\omega_0/[\ln|\gamma_T|-\psi(\tfrac{1}{2})] \ . \quad (36b)$$

These equations show that the spacing does not vanish, as does the classical orbit frequency, but instead is lower than a typical classical frequency (e.g., ω_0) by only a factor of the order of the logarithm of the number of trapped quantum states.

Considerable simplification results when the potential is symmetric. In this case, the states can be classified according to parity, and Eq. (24) becomes

$$\cos(\pi I_T-\varphi)=-[1+\exp(2\pi\gamma)]^{-1/2} \ . \quad (37)$$

For large, positive γ, the right side of this equation vanishes, and so the quantization condition (29) is obtained as before. For large, negative γ, the right side asymptotes to -1. Hence, the solutions are nearly degenerate roots at

$$I_+ \approx (n+\tfrac{1}{2})h \ , \quad (38)$$

but split by the exponentially small deviation of the right side of (37) from -1. Of the two corresponding eigenstates, one is even, and the other is odd. The two states are not localized in either well, but have the same amplitudes in the two wells for the even case and opposite amplitudes for the odd case. For $\gamma \lesssim 1$ the result analogous to (35) is

$$\cos\{\pi N_T+\gamma[\ln|\gamma_T|-\psi(\tfrac{1}{2})]\}=-(1+e^{2\pi\gamma})^{-1/2} \ , \quad (39)$$

which again shows that the states have a separation given by Eq. (32).

These results indicate that quantum effects strongly modify the interaction of such systems. A classical system most strongly interacts with an external force that is in resonance, i.e., has a frequency equal to the classical orbit frequency. Thus, we may say that the classical excitation frequency is the orbit frequency. A quantum system interacts strongly with external forces of frequencies equal to the frequency differences. In analogy, the quantum excitation frequency is the frequency difference between states. These excitation frequencies agree in the semiclassical limit, as they should. However, Eq. (36b) indicates that for states near the separatrix, the semiclassical limit requires that the logarithm of the number of quantum states be large. This is a much more stringent condition than the usual one that simply requires the number of states be large. This indicates that quantum effects may be observable even in macroscopic systems by examining the dynamics of states near the separatrix.

III. RELATIVE PROBABILITIES

In the previous section, the relations between the wave-function amplitudes for the various regions were obtained. This is sufficient to obtain the energy spectrum. However, for integration of the rotating-frame equations [30], for example, matrix elements of the normalized wave functions are needed. In this section we show how to obtain these normalization factors. The amplitudes needed to have normalized wave functions were previously obtained by Yngve [22]. However, the present analysis allows one to see the contributions to the normalization from the various parts of the wave function. Moreover, we give the values of the WKB amplitudes in the regions 1 and 3, where the rapidly varying phase approximation is valid. These are the most convenient for taking the classical limit.

As just mentioned, we will use the normalization condition to obtain the value of the mean-square amplitudes,

$$A \equiv \sqrt{A_+^2+A_-^2} \ , \quad (40)$$

of regions 1 and 3. The amplitude (40) may be expressed in terms of the norm

$$\Xi \equiv \int_{-\infty}^{\infty} dx\,|\phi|^2/A^2 \quad (41a)$$

of the unnormalized wave function. The requirement that ϕ be normalized gives

$$A=1/\Xi^{1/2} \ . \quad (41b)$$

As usual, the overall phase is irrelevant. From the amplitude (41b) and the Eqs. (22) and (40) the wave amplitudes for both sides of the potential follow immediately. The ratios are

$$\left[\frac{A_\pm}{A}\right]^2=\frac{\cos^2(\theta_\mp)}{\cos^2(\theta_\mp)+\kappa^2\sin^2(\theta_\pm)} \ . \quad (42)$$

The relative sign of A_+ and A_- is determined from (18a) for a particular wave function, i.e., particular value of γ.

Equation (42) shows explicitly how deeply trapped wave functions are localized on one side of the barrier. For example, for the sequence $I_+=(n+1/2)h$ of Eq. (28), which corresponds to $\cos(\theta_+)=0$ of Eq. (26), Eq. (42) implies that A_-/A vanishes. Thus, wave functions corresponding to quantization of the action to the left of the barrier have no (or exponentially small) amplitude in the right barrier.

The normalization integral can be written as a sum of two parts,

$$\Xi=A_+^2\,\Xi_+/A^2+A_-^2\,\Xi_-/A^2 \ , \quad (43a)$$

with

$$\Xi_+ \equiv \int_0^\infty dx\,|\phi|^2/|A_+|^2 \tag{43b}$$

and

$$\Xi_- \equiv \int_{-\infty}^0 dx\,|\phi|^2/|A_-|^2 \ . \tag{43c}$$

The integrals of (43b) and (43c) once calculated, together with Eq. (42), determine the normalization integral (40), which in turn determines the amplitude (41). Given either of the integrals (43b) or (43c), the other follows readily. Thus, we now concentrate on the calculation of (43b).

In the case where the energies are far from the separatrix, the normalization integrals are more easily calculated. They are given by the integrals (43) limited to the region between the turning points. In these integrals the usual rapidly varying phase functions (8) are used. The singularity ($\sim 1/\sqrt{x}$) of the square of these functions near a linear turning point is not a problem as this singularity is integrable. However, for energy equal to that of the separatrix, the square of the WKB wave functions diverges more strongly ($\sim 1/x$), such that the integral no longer converges. This indicates that the central region 2 will influence the normalization integrals for energy close to the separatrix energy. It is this case that we now turn to.

To calculate the integral (43b), the integration is divided into two parts,

$$\Xi_+ = \Xi_{2+} + \Xi_{3+} \ , \tag{44}$$

each corresponding to a portion of the real line as shown in Fig. 2. In particular,

$$\Xi_{2+} = \int_0^{y_+} dx\,|\phi|^2/A_+^2 \ , \tag{45a}$$

where y_+ is in the overlap region (17), and

$$\Xi_{3+} = \int_{y_+}^\infty dx\,|\phi|^2/A_+^2 \ . \tag{45b}$$

The exact choice of the end point y_+ of the integrals must be irrelevant, if the asymptotic theory is correct. In fact, we would like to write these results in such a way as to make manifest the independence of the normalization on the limit y_+.

To calculate the integral (45b) we must insert the uniform Airy solution, which we have not given. We have given only the rapidly varying phase solutions (8). However, beyond the right turning point, the Airy solutions become exponentially small. In addition, the region surrounding the outer turning point where the Airy solutions differ significantly from the rapidly varying phase solutions has a width that is $O(\hbar^{2/3})$, and there the Airy functions reach a magnitude that is only $O(\hbar^{-1/6})$. Thus, the contribution of this region to the integral is small in the limit $\hbar \to 0$ and can be ignored. As a result, we can replace the upper bound in the integral (45b) by the right turning point and use the rapidly varying phase solution

$$\Xi_{3+} = \int_{y_+}^{x_+} dx\,\sin^2\left[\hbar^{-1}\int_x^{x_+} p(y)dy + \pi/4\right] \Big/ |Q|^{1/2} \ .$$

That the upper singularity is integrable is another manifestation of the unimportance of the region near and beyond the outer turning point. In this integral the square of the sine yields two terms, as $\sin^2\alpha = [1-\cos(2\alpha)]/2$. The term $\cos(2\alpha)$ has a rapidly varying phase and, so, vanishes as $\hbar \to 0$. Therefore,

$$\Xi_{3+} = \tfrac{1}{2}\int_{y_+}^{x_+} dx/p(x) \ . \tag{46}$$

This is the usual semiclassical result: The contribution to the normalization integral of some region dx of the real line is proportional to the time $dt = m\,dx/p$ that would be spent in this region by a classical particle.

We can simplify Eq. (46) by setting the energy to zero, because unlike the barrier region, in the region of the integral (46) the wave-function amplitude is not sensitive to the energy. To evaluate this integral, we add and subtract the term that is singular at the origin. Thus, we obtain

$$\Xi_{3+} = \tfrac{1}{2}\int_{y_+}^{s_+} dx \left[\frac{1}{|2mV(x)|^{1/2}} - \frac{1}{|mb|^{1/2}x}\right] + \tfrac{1}{2}\int_{y_+}^{s_+} \frac{dx}{|mb|^{1/2}x} \ .$$

The lower limit of the first integral in this equation may be replaced by zero, since it is not singular at the origin, and y_+ is small. Then this integral may be evaluated with the use of Eq. (31). The second integral of this expression is simply a logarithm. Therefore, we obtain

$$\Xi_{3+} = \tfrac{1}{4}|mb|^{-1/2}\ln|E_+/2by_+^2| = \tfrac{1}{4}|mb|^{-1/2}\ln|\gamma_+/\eta_+^2| \ , \tag{47}$$

in which the definition

$$\eta_+ \equiv \Lambda y_+ \tag{48}$$

has been used. The expression (47) isolates the dependence of the integral on its lower limit. As we shall see, this dependence is canceled by a corresponding dependence in Ξ_{2+}.

The calculation of Ξ_{2+} begins with the insertion of Eq. (13) into (45a) and the use of the relations (18) to eliminate the amplitudes C and D in favor of the amplitude A_+. This calculation is facilitated by the introduction of Whittaker's function, which is related to the parabolic cylinder functions via

$$D_{i\gamma-1/2}(\eta e^{-i\pi/4}) = \frac{1}{\sqrt{2}}\exp\left[\frac{\pi\gamma}{4} - \frac{i\pi}{8} + \frac{i}{2}\arg[\Gamma(\tfrac{1}{2}+i\gamma)]\right][\kappa^{-1/2}W(-\gamma,\eta) + i\kappa^{1/2}W(-\gamma,-\eta)] \ . \tag{49}$$

This relation may be derived from Ref. [39], Eqs. 19.3.1, 19.17.6, and 19.17.7. In addition, the scaled variable η is used for the integration. This procedure gives

$$\Xi_{2+}=\frac{e^{-\pi\gamma/2}}{4\sqrt{mb}}\int_0^{\eta_+}d\eta[e^{i\pi/8-i\pi N_+-i(\gamma/2)\ln|\gamma_+|}D_{i\gamma-1/2}(\eta e^{-i\pi/4})+\text{c.c.}]^2$$

$$=\frac{e^{-\pi\gamma/2}}{4\sqrt{mb}}\left[e^{i\pi/4-i2\pi N_+-i\gamma\ln|\gamma_+|}\int_0^{\eta_+}d\eta\,D^2_{i\gamma-1/2}(\eta e^{-i\pi/4})\right.$$

$$\left.+\int_0^{\eta_+}d\eta\,D_{i\gamma-1/2}(\eta e^{-i\pi/4})D_{-i\gamma-1/2}(\eta e^{i\pi/4})\right]+\text{c.c.} \tag{50}$$

The second integral can be converted to a more easily evaluated form by using the relation,

$$D_{-i\gamma-1/2}(\eta e^{i\pi/4})=\frac{\Gamma(\frac{1}{2}-i\gamma)}{\sqrt{2\pi}}[e^{-\pi\gamma/2+i\pi/4}D_{i\gamma-1/2}(\eta e^{-i\pi/4})+e^{\pi\gamma/2-i\pi/4}D_{i\gamma-1/2}(-\eta e^{-i\pi/4})]\ .$$

Insertion of this relation yields

$$\Xi_{2+}=\frac{e^{-\pi\gamma/2}}{4\sqrt{mb}}\left[e^{i\pi/4}\left[e^{-i2\pi N_+-i\gamma\ln|\gamma_+|}+\frac{\Gamma(\frac{1}{2}-i\gamma)}{\sqrt{2\pi}}e^{-\pi\gamma/2}\right]L_1+\frac{\Gamma(\frac{1}{2}-i\gamma)}{\sqrt{2\pi}}e^{\pi\gamma/2-i\pi/4}L_2\right]+\text{c.c.}\ ,$$

in which the definitions (A1) and (B1) have been used. These integrals are calculated in Appendixes A and B. Combining this equation with (A4) and (B7) yields

$$\Xi_{2+}=\frac{1}{2\sqrt{mb}}\ln|\eta_+|-\frac{1}{4\sqrt{mb}}\text{Re}[\psi(\tfrac{1}{2}+i\gamma)]$$

$$-\frac{e^{-\pi\gamma/2}}{8\sqrt{mb}}\text{Im}\left\{\left[\frac{\sqrt{2\pi}}{\Gamma(\frac{1}{2}-i\gamma)}e^{-i2\pi N_+-i\gamma\ln|\gamma_+|}+e^{-\pi\gamma/2}\right]\left[\psi\left[\frac{3}{4}-\frac{i\gamma}{2}\right]-\psi\left[\frac{1}{4}-\frac{i\gamma}{2}\right]\right]\right\}\ . \tag{51}$$

This equation shows that the contribution of the barrier region to the normalization integral need not scale with Planck's constant. The first term diverges logarithmically with the scaled matching point, but the scaled matching point need only be large compared with unity, according to Eqs. (16), (17), and (48), not necessarily large compared with some inverse power of Planck's constant. The remaining terms are also seen to be of order unity for γ of order unity.

We now have a complete picture of the relative probability of being in the various regions. The contribution of the near-barrier region, which is the small-x part of the complement of the region (17) where the rapidly varying phase solution breaks down, is of order unity, as is the contribution of the region where x is $O(1)$. It is the contribution of the intermediate region (17) that gives the dominant contribution.

We add Ξ_{2+} and Ξ_{3+} to obtain the normalization integral over the positive x axis. The terms containing $\ln|\eta_+|$ cancel, as they must, since the analysis cannot depend on the choice of matching points. Below we give the result for both Ξ_+ and Ξ_-

$$\Xi_\pm=\frac{\ln|\gamma_\pm|-\text{Re}[\psi(\frac{1}{2}+i\gamma)]}{4\sqrt{mb}}+\frac{\pi\sqrt{2\,\text{sech}(\pi\gamma)}\sin(2\theta_\pm)e^{-\pi\gamma/2}}{8\sqrt{mb}}$$

$$-\frac{e^{-\pi\gamma}}{8\sqrt{mb}}\left\{2\,\text{Im}\left[\psi\left[\frac{1}{4}+\frac{i\gamma}{2}\right]\right]-\pi\tanh(\pi\gamma)\right\}[1+e^{\pi\gamma/2}\sqrt{2\cosh(\pi\gamma)}\cos(2\theta_\pm)]\ . \tag{52}$$

Identities for the ψ function and our relations (19) and (20) for the angles $\theta_\pm$ were used to obtain Eq. (52). The complete normalization constant is obtained by inserting Eqs. (52) and (42) into Eq. (43a). Several terms, including all of those in the brackets of (52), cancel after combination and use of the dispersion relation (23). The result is

$$\Xi=\frac{1}{4m^{1/2}\omega_0}\sum_{j=\pm}\left[\frac{A_j}{A}\right]^2\left[\ln|\gamma_j|-\text{Re}[\psi(\tfrac{1}{2})+i\gamma]+\frac{\pi\sin(\theta_j)\cos(\theta_j)e^{-\pi\gamma/2}}{\sqrt{e^{\pi\gamma}+e^{-\pi\gamma}}}\right] \tag{53a}$$

$$=\frac{\ln|\gamma_T|-\text{Re}[\psi(\frac{1}{2}+i\gamma)]}{4m^{1/2}\omega_0}+\frac{\ln|\gamma_+/\gamma_-|\sin(\theta_\Delta)+\pi e^{\pi\gamma}\text{sech}(\pi\gamma)\cos(\theta_\Delta)}{8m^{1/2}\omega_0\sin(\theta_T)\sqrt{1+e^{2\pi\gamma}}}\ . \tag{53b}$$

The quantities θ_T and θ_Δ were defined in Eqs. (25).

For the symmetric case, Eq. (53) reduces via the relation, $\sin(\theta_T)=\pm(1+e^{-2\pi\gamma})^{-1/2}$, derivable from Eq. (3), to

$$\Xi=\frac{\ln|\gamma_T|-\text{Re}[\psi(\frac{1}{2}+i\gamma)]}{4\sqrt{mb}}\pm\frac{\pi\,\text{sech}(\pi\gamma)}{8\sqrt{mb}}\ , \tag{54}$$

where the sign is given by the parity of the state, i.e., $A_-=\pm A_+$. For γ of order unity, the first two contributions to the normalization are positive. The last contribution is positive (negative) for states of positive (negative) parity. This arises because the negative-parity states must vanish at the origin, and so the contribution of the near-origin region to the normalization will be smaller.

As must be the case, the normalizations (53) and (54) are finite for any value of γ provided $\hbar$ does not vanish. [The quantity $\sin(\theta_T)$ in the denominator of the last term of (53) cannot vanish, as Eq. (24) indicates that $\cos(\theta_T)$ has a magnitude less than unity.] However, Eqs. (53) and (54) indicate that the normalization constant diverges logarithmically for fixed γ in the limit $\hbar \to 0$, because in this limit $\gamma_T = O(1/\hbar)$. The reason is that in this limit, the classical probability density becomes singular on the separatrix, because the particle spends all of its time at the x point. Quantum effects regularize this singularity. The quantum probability density no longer diverges, but the probability of not being near the barrier approaches zero logarithmically with Planck's constant.

The quantum modifications disappear for γ greater than or of order unity. For the symmetric case (55) the last term is exponentially small for large γ. Since $\psi(z) \sim \ln|z|$ for large z, the first two terms reduce to $\ln|E_T/E|/2m^{1/2}\omega_0$, which according to the discussion just after Eq. (31), is one-fourth of the sum of the classical periods of the left and right wells divided by the square root of the mass. The factor is seen in Eq. (46). One half is the prefactor due to locally averaging $\sin^2$. Another half comes from the quantum integral being one integration between turning points, while for the classical period one must integrate from one turning point to the other and back. The divisor of $m^{1/2}$ arises because our normalization led to $p(x)$ being in the denominator rather than $v(x) = p(x)/m^{1/2}$ as would be the case in the integral for the classical period.

A similar disappearance of the quantum effects is seen in the asymmetric case. For large, positive γ, the last term in Eq. (53b) is small, and so the first two terms reduce to $\ln|E_T/E|/2m^{1/2}\omega_0$, as before. For large, negative γ wave functions trapped in, say, the positive well, A_-/A is exponentially small, and A_+/A goes to unity, so that only the $j = +$ term in the sum is important. For this term, the last term in the brackets vanishes: The exponentials in the numerator and denominator cancel, and the cosine is exponentially small, according to our discussion of Eq. (42). Thus, for wave functions trapped in the positive well, the normalization constant is $\ln|E_+/E|/4m^{1/2}\omega_0$, or one-fourth of the classical period for a particle trapped in the right well.

Figure 3 shows a typical near-separatrix wave function. Far from the barrier the rapidly varying phase approximation applies. Thus, the wave function is given by Eqs. (8), where according to Eqs. (46) and (54), the amplitude is $O(1/\ln|1/\hbar|)$. On the barrier side of this region the parabolic cylinder functions apply. Equations (18) show that these functions rise to an amplitude that is $O(1/\hbar^{1/4})$, so that the probability of being in this region is order unity.

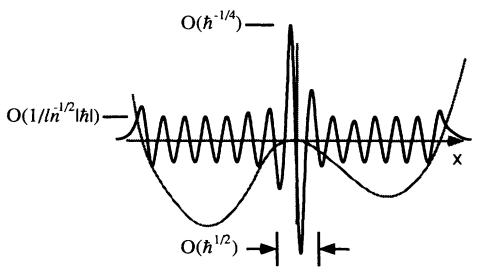

FIG. 3. A typical near-separatrix wave function.

IV. MATRIX ELEMENTS

Matrix elements are needed to calculate the transition probabilities between states. In particular the matrix elements of the time derivative $\partial_t H$ of the Hamiltonian are needed for the transformation to the rotating-frame basis, which is used in the study of the loss of quantum adiabaticity in systems with a separatrix. In this section we discuss the calculation of matrix elements for macroscopic functions of position. That is, we consider the matrix elements of a function $U(x)$ that varies on the same scale as the potential.

The first step in calculating this matrix element is to add and subtract the value of U at the unstable fixed point,

$$U(x) = U(x) - U(0) + U(0) .$$

Insertion of this result into the matrix element yields

$$\langle \phi_k | U | \phi_j \rangle = \delta_{kj} U(0) + \langle \phi_k | U - U(0) | \phi_j \rangle , \tag{55}$$

because the matrix elements are orthonormal. (It is now necessary to restore the subscripts referring to the quantum state.) The first term in (55) is simply a shift of the energy levels. For the remainder we define the matrix elements M_{kj} via

$$M_{kj} = \frac{\langle \phi_k | U - U(0) | \phi_j \rangle}{A_k A_j} , \tag{56}$$

where the quantity A_j is the value for state j of the amplitude A that appears in, for example, Eqs. (40)–(42). Thus, the elements M_{kj} are calculated with the unnormalized wave functions. In this section we calculate these elements M_{kj}.

Taylor expansion shows that near the unstable fixed point, the function in the matrix element (56) has the form,

$$U(x) - U(0) = U'(0)x + O(x^2) . \tag{57}$$

The linearity of this function in x near the origin counteracts the $1/x$ singularity of the wave functions (8) at the origin. Thus, the integrand of the numerator of (56) is finite. This implies that region 2 does not contribute to this integral, because its width vanishes with $\hbar$, and the integrand is finite. Only regions 1 and 3, where the rapidly varying phase approximation is valid, contribute.

In keeping with the last section, we write the integral in the form,

$$M_{jk} = \frac{A_{j+} A_{k+}}{A_j A_k} M_{jk+} + \frac{A_{j-} A_{k-}}{A_j A_k} M_{jk-} , \tag{58a}$$

where

$$M_{jk\pm}\equiv\pm\frac{1}{A_{j\pm}A_{k\pm}}\int_0^{\pm\infty}dx\,\phi_k[U(x)-U(0)]\phi_j\ . \quad (58b)$$

(We have chosen the eigenfunctions to be real.) The quantities $A_{j\pm}$ are the amplitudes $A_\pm$ for the eigenmode j. After calculating M_{jk+}, M_{jk-} will follow immediately.

Use of Eq. (8b) and (58b) yields the result,

$$M_{jk+}\equiv\int_{a_{+jk}}^{x_{+jk}}dx\frac{U(x)-U(0)}{\sqrt{p_jp_k}}\times\sin\left[\frac{1}{\hbar}\int_x^{x_+}p_j(x')dx'+\frac{\pi}{4}\right]\times\sin\left[\frac{1}{\hbar}\int_x^{x_+}p_k(x')dx'+\frac{\pi}{4}\right], \quad (59)$$

in which a_{+jk} is the greater of the interior turning points for the energies E_j and E_k, and x_{+jk} is the lesser of the outer turning points for these energies. These choices are not critical, because the integrand is bounded near the origin and integrable at the outer turning point. Hence, the error by making a different choice for the integration limits is less than $O(1)$. The quantities p_j are the classical momenta corresponding to these energies, i.e.,

$$p_j(x)=\sqrt{2mE_j-2mV(x)}\ , \quad (60)$$

in agreement with Eq. (2b).

Combining the sines in Eq. (59) yields a cosine of the sum of the arguments and a cosine of the difference. The cosine of the sum is a rapidly varying function that integrates to zero in the limit of small $\hbar$. Hence, this integral is not important. We are left with

$$M_{jk+}\equiv\tfrac{1}{2}\int_{a_{+jk}}^{\infty}dx\frac{U(x)-U(0)}{\sqrt{p_jp_k}}\times\cos\left[\frac{1}{\hbar}\int_x^{x_+}p_j(x')dx'-\frac{1}{\hbar}\int_x^{x_+}p_k(x')dx'\right]. \quad (61)$$

To evaluate the momenta in (61) we use Taylor expansion of (60),

$$p_j(x)\approx p_x(x)+\frac{mE_j}{p_x(x)}\ ,$$

where

$$p_x(x)\equiv\sqrt{-2mV(x)} \quad (62)$$

is the momentum for the separatrix trajectory. This expansion breaks down near the maximum. But this is unimportant as before, because the region of breakdown is small, and the integrand is finite. For the numerator of the integrand we need only the first term of the Taylor expansion. Upon inserting these relations, no additional error is incurred by setting the lower limit of the integral to zero and the upper limit to the outer turning point of the separatrix. Thus, we obtain

$$M_{jk\pm}\equiv\tfrac{1}{2}\int_0^{s_\pm}dx\frac{U(x)-U(0)}{p_x(x)}\times\cos\left[m\frac{E_j-E_k}{\hbar}\int_x^{s_\pm}dx'/p_x(x')\right], \quad (63)$$

the result for both wells. The total matrix element is obtained by inserting (63) and (22a) into Eq. (58a). In the general case, this yields

$$M_{jk}=\frac{A_{j+}A_{k+}}{2A_jA_k}\int_0^{s_+}dx\frac{U(x)-U(0)}{p_x(x)}\cos\left[m\frac{E_j-E_k}{\hbar}\int_x^{s_\pm}dx'/p_x(x')\right]+\frac{A_{j-}A_{k-}}{2A_jA_k}\int_{s_-}^{0}dx\frac{U(x)-U(0)}{p_x(x)}\cos\left[m\frac{E_j-E_k}{\hbar}\int_{s_-}^{x}dx'/p_x(x')\right]. \quad (64a)$$

For the symmetric case this result simplifies to

$$M_{jk}=\tfrac{1}{2}\int_0^{s_+}dx\frac{U(x)-U(0)}{p_x(x)}\times\cos\left[m\frac{E_j-E_k}{\hbar}\int_x^{s_+}dx'/p_x(x')\right], \quad (64b)$$

if the two states have the same parity, while

$$M_{jk}=0 \quad (64c)$$

if the states are of opposite parity.

In contrast with the normalization factors, the unnormalized matrix elements for states near the separatrix do not diverge in the limit $\hbar\to0$. The integrand is bounded because the $1/p$ singularity is canceled by the vanishing (57) of $U(x)-U(0)$ near the origin. The phase of the cosine diverges as $1/x\ln|1/\hbar|$, because the energy difference (52b) scales as $\hbar/\ln|1/\hbar|$, but the cosine is bounded. Moreover, the contribution of the near-origin region is small because the oscillations of the cosine are arbitrarily rapid near the origin. This indicates that the major contribution to the unnormalized matrix element comes from the region far from the x point.

V. SUMMARY AND CONCLUSIONS

We have discussed the probability density and shown how the matrix elements for macroscopic functions of position may be calculated for near-separatrix eigenfunctions. Our analysis of the normalization constant shows that the probability of being far from the s point vanishes logarithmically with Planck's constant. Thus, it approaches the classical limit (zero) very slowly. Our analysis of the matrix elements shows that the region near the fixed point does not contribute to the unnormalized elements. Thus, the quantum resolution of the classical divergence is only through the wave-function normalizations.

This work provides a basis for the calculation of transition probabilities between separatrix states due to perturbing forces. It also provides a basis for the calculation of the loss of the quantum adiabatic invariant [30].

ACKNOWLEDGMENTS

We gratefully acknowledge useful discussions with Rex Skodje, David Bruhwiler, and Robert Littlejohn. This work was supported by the U.S. Department of Energy under Grant No. DE-FG02-85ER53207.

APPENDIX A: EVALUATION OF THE INTEGRAL L_1

In this section, we calculate the integral,

$$L_1 \equiv \int_0^{\eta_+} d\eta\, D^2_{i\gamma-1/2}(\eta e^{-i\pi/4}) , \tag{A1}$$

which is needed for the development of Sec. III. To evaluate L_1, we introduce the auxiliary variable $\tau \equiv \eta e^{-i\pi/4}$. Thus, the integration is along the ray $\arg(\tau) = -\pi/4$. We deform this contour as shown in Fig. 4 to be first along the real-τ axis, then along a circular arc to $\tau \equiv \eta_+ e^{-i\pi/4}$. We obtain

$$L_1 \equiv e^{i\pi/4}\left[\int_0^{\eta_+} d\tau\, D^2_{i\gamma-1/2}(\tau) + \int_{\eta_+}^{\eta_+ e^{-i\pi/4}} d\tau\, D^2_{i\gamma-1/2}(\tau)\right] . \tag{A2}$$

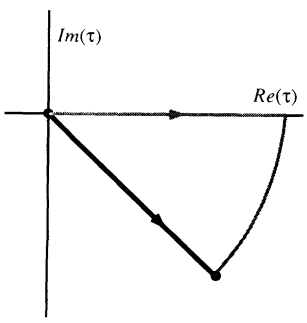

FIG. 4. Contour modification for the integral (A2). The original integration contour in the complex-τ plane is the darker line. The deformed contour (lightly drawn) is composed of a piece along the real-τ axis and an arc of angle $\pi/4$ at large τ.

The asymptotic form for $\tau \gg |\gamma|$ of Whittaker's function is found from Eqs. 19.3.1 and 19.8.1 of Ref. [39]. The result is

$$D_{i\gamma-1/2}(\tau) \sim e^{-\tau^2/2}\tau^{i\gamma-1/2} . \tag{A3}$$

Hence, the integrands in (A2) are exponentially small for large τ, and the second integral may be ignored. For the same reason the upper limit of the first integral may be set to ∞. With this, the first integral may be found in [Ref. 43], p. 885. The result is

$$L_1 \equiv \tfrac{1}{2}\sqrt{\pi/2}\,e^{i\pi/4}\frac{\psi\left[\frac{3}{4}-\frac{i\gamma}{2}\right]-\psi\left[\frac{1}{4}-\frac{i\gamma}{2}\right]}{\Gamma(\frac{1}{2}-i\gamma)} . \tag{A4}$$

APPENDIX B: EVALUATION OF THE INTEGRAL L_2

In the development of Sec. IV, the integral

$$L_2 \equiv \int_0^{\eta_+} d\eta\, D_{i\gamma-1/2}(\eta e^{-i\pi/4}) \times D_{i\gamma-1/2}(-\eta e^{-i\pi/4}) \tag{B1}$$

is needed for large η_+. In this appendix we evaluate this integral. We do so by introducing the auxiliary variable $\tau \equiv \eta e^{-i\pi/4}$ and modifying the contour of integration as in Fig. 4. Thus, we obtain

$$L_2 = e^{i\pi/4}(L_{2a} + L_{2b}) , \tag{B2}$$

where

$$L_{2a} \equiv \int_0^{\eta_+} d\tau\, D_{i\gamma-1/2}(\tau) D_{i\gamma-1/2}(-\tau) \tag{B3a}$$

and

$$L_{2b} \equiv \int_{\eta_+}^{\eta_+ e^{-i\pi/4}} d\tau\, D_{i\gamma-1/2}(\tau) D_{i\gamma-1/2}(-\tau) . \tag{B3b}$$

The integral (B3a) diverges as $\eta_+ \to \infty$. To extract this behavior we set the index of the first Whittaker function to γ'. In this case the integral over the infinite domain can be found. We subtract the added portion of the integral. Then we take the limit $\gamma' \to \gamma$.

The asymptotic form of the integrand for differing indices may be obtained from Eqs. 19.3.1, 19.4.2, 19.8.1, and 19.8.2 of Ref. [39]. The result is

$$D_{i\gamma'-1/2}(\tau) D_{i\gamma-1/2}(-\tau) \sim \frac{\sqrt{2\pi}}{\Gamma(\frac{1}{2}-i\gamma)}\tau^{i(\gamma'-\gamma)-1} . \tag{B4}$$

Thus,

$$L_{2a} = \lim_{\gamma' \to \gamma}\left[\int_0^{\infty} d\tau\, D_{i\gamma'-1/2}(\tau) D_{i\gamma-1/2}(-\tau) - \frac{\sqrt{2\pi}}{\Gamma(\frac{1}{2}-i\gamma)}\int_{\eta_+}^{\infty} d\tau\, \tau^{i(\gamma'-\gamma)-1}\right] .$$

The first integral in this expression can be found in Ref. 42, p. 885. The second integral is trivially found. This gives

$$iL_{2a}/\sqrt{2\pi}=\lim_{\gamma'\to\gamma}\left\{\frac{\dfrac{\eta_+^{i(\gamma'-\gamma)}}{\Gamma(\frac{1}{2}-i\gamma)}-\sqrt{\pi}2^{i(\gamma'+\gamma-1)/2}\left[\dfrac{1}{\Gamma(\frac{3}{4}-i\gamma/2)\Gamma(\frac{1}{4}-i\gamma'/2)}+\dfrac{1}{\Gamma(\frac{3}{4}-i\gamma'/2)\Gamma(\frac{1}{4}-i\gamma/2)}\right]}{\gamma'-\gamma}\right\}.$$

The numerator and denominator in this expression vanish as $\gamma'\to\gamma$. Therefore, we obtain the result by L'Hôpital's rule. This gives

$$L_{2a}=\frac{\sqrt{2\pi}}{\Gamma(\frac{1}{2}-i\gamma)}\{\tfrac{1}{2}\ln|\eta_+^2/2| -\tfrac{1}{4}[\psi(\tfrac{1}{4}-i\gamma/2)+\psi(\tfrac{3}{4}-i\gamma/2)]\}\ . \tag{B5}$$

The second part L_{2b} is straightforwardly integrated. We find

$$L_{2b}=\frac{-i\pi}{4}\frac{\sqrt{2\pi}}{\Gamma(\frac{1}{2}-i\gamma)}\ . \tag{B6}$$

The entire integral L_2 is found by inserting (B5) and (B6) into (B2). The result is

$$L_2=e^{i\pi/4}\frac{\sqrt{2\pi}}{\Gamma(\frac{1}{2}-i\gamma)}\{\tfrac{1}{2}\ln|\eta_+^2/2| -\tfrac{1}{4}[\psi(\tfrac{1}{4}-i\gamma/2) +\psi(\tfrac{3}{4}-i\gamma/2)+i\pi]\}\ .$$

Finally, we use Eq. 6.3.8 of Ref. [39] to obtain

$$L_2=\frac{\sqrt{2\pi}e^{i\pi/4}}{\Gamma(\frac{1}{2}-i\gamma)}\left[\ln|\eta_+|-\tfrac{1}{2}\psi(\tfrac{1}{2}-i\gamma)-\frac{i\pi}{4}\right]. \tag{B7}$$

*Also at Department of Astrophysical, Planetary, and Atmospheric Science, University of Colorado, Boulder, CO 80309-0390.

†Present address: Thinking Machines Corporation, 245 First Street, Cambridge, MA 02142-1264.

[1] *Hamiltonian Dynamical Systems,* edited by R. S. MacKay and J. D. Meiss (Hilger, Bristol, England, 1987).
[2] A. J. Lichtenberg and M. A. Lieberman, *Regular and Stochastic Motion* (Springer-Verlag, New York, 1983).
[3] G. M. Zaslavski, Phys. Rep. **80**, 157 (1981).
[4] N. Pomphrey, J. Phys. B **7**, 1909 (1974).
[5] I. C. Percival, Adv. Chem. Phys. **36**, 1 (1977).
[6] M. V. Berry, Philos. Trans. R. Soc. London, Ser. A **287**, 237 (1977); J. Phys. A **10**, 2083 (1977).
[7] G. M. Zaslavskii, Zh. Eksp. Teor. Fiz. **73**, 2089 (1979) [Sov. Phys. JETP **46**, 1094 (1977)].
[8] S. W. McDonald, Phys. Rev. Lett. **42**, 1189 (1979).
[9] F. M. Izrailev and D. L. Shepelyanski, Theor. Math. Phys. **43**, 417 (1983).
[10] S. Fishman, D. R. Grempel, and R. E. Prange, Phys. Rev. Lett. **49**, 509 (1982).
[11] V. K. Melnikov, Trans. Moscow Math. Soc. **12**, 1 (1963).
[12] M. V. Berry and K. E. Mount, Rep. Prog. Phys. **32**, 315 (1972).
[13] D. L. Hill and J. A. Wheeler, Phys. Rev. **89**, 102 (1953).
[14] K. W. Ford, D. L. Hill, M. Wakano, and J. A. Wheeler, Ann. Phys. (N.Y.) **7**, 239 (1959).
[15] N. Fröhman, Ark. Fys. **32**, 79 (1966).
[16] J. N. L. Connor, Mol. Phys. **15**, 37 (1968); Chem. Phys. Lett. **4**, 419 (1969).
[17] T. Y. Wu, Phys. Rev. **44**, 727 (1933).
[18] N. Fröman, Ark. Fys. **32**, 541 (1966).
[19] R. Paulsson, F. Karlsson, and R. J. LeRoy, J. Chem. Phys. **79**, 4346 (1983).
[20] J. R. Cary, P. Rusu, and R. T. Skodje, Phys. Rev. Lett. **58**, 292 (1987).
[21] J. R. Cary, D. F. Escande, and J. L. Tennyson, Phys. Rev. A **34**, 4256 (1986).
[22] S. Yngve, J. Math. Phys. **13**, 324 (1972).
[23] W. H. Furry, Phys. Rev. **71**, 366 (1947).
[24] R. Paulsson and N. Fröman, Ann. Phys. (N.Y.) **163**, 227 (1985).
[25] C. R. Menyuk, Phys. Rev. A **31**, 3282 (1985).
[26] A. V. Timofeev, Zh. Eksp. Teor. Fiz. **75**, 1303 (1978) [Sov. Phys. JETP **48**, 656 (1978)].
[27] V. Ya. Davydovskii and A. I. Matveev, Zh. Tekh. Fiz. **53**, 2125 (1983) [Sov. Phys. Tech. Phys. **28**, 1302 (1983)].
[28] A. I. Neishtadt, Sov. J. Plasma Phys. **12**, 568 (1986) [Fiz. Plazmy **12**, 992 (1986)].
[29] A. Messiah, *Quantum Mechanics* (North-Holland, Amsterdam, 1958), Vol. II, p. 745.
[30] J. R. Cary and P. Rusu (unpublished).
[31] P. Rusu, Ph.D. thesis, University of Colorado, 1990.
[32] L. S. Brown and G. Gabrielse, Rev. Mod. Phys. **58**, 233 (1986), and references therein.
[33] A. R. Mickelson, I. P. Januar, P. Rusu, and J. R. Cary, in *Proceedings of the National Radio Science Meeting, Boulder, 1990* (National Academies of Science and Engineering, National Research Council, Boulder, 1990), p. 157.
[34] M. J. Davis, J. Phys. Chem. **92**, 3124 (1988).
[35] R. E. Langer, Phys. Rev. **51**, 669 (1937).
[36] P. Pechukas, J. Chem. Phys. **54**, 3864 (1971).
[37] H. Moriguchi, J. Phys. Soc. Jpn. **14**, 1771 (1959).
[38] S. C. Miller and R. H. Good, Jr., Phys. Rev. **91**, 174 (1953).
[39] C. M. Bender and S. Orzsag, *Advanced Mathematical Methods for Scientists and Engineers* (McGraw-Hill, New York, 1978).
[40] *Handbook of Mathematical Functions,* edited by M. Abramowitz and I. A. Stegun (Dover, New York, 1965).
[41] N. Fröman, P. O. Fröman, U. Myhrman, and R. Paulsson, Ann. Phys. (N.Y.) **74**, 314 (1972).
[42] C. Zener, Proc. R. Soc. London, Ser. A **137**, 696 (1932).
[43] I. S. Gradshteyn and I. M. Ryzhik, Table of Integrals, Series and Products (Academic, New York, 1980).

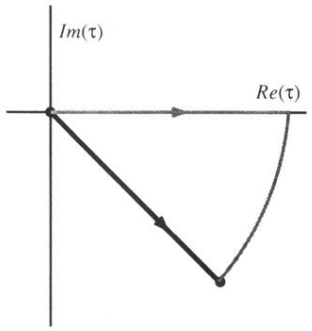

FIG. 4. Contour modification for the integral (A2). The original integration contour in the complex-τ plane is the darker line. The deformed contour (lightly drawn) is composed of a piece along the real-τ axis and an arc of angle $\pi/4$ at large τ.